

International Conference on Space Optics—ICSO 2012

Ajaccio, Corse

9–12 October 2012

Edited by Bruno Cugny, Errico Armandillo, and Nikos Karafolas



Study of photonic resonant angular velocity sensors as alternative gyro technology

C. Ciminelli

F. Dell'Olio

C. E. Campanella

M. N. Armenise

et al.



Study of photonic resonant angular velocity sensors as alternative gyro technology

C. Ciminelli, F. Dell'Olivo, C. E. Campanella, M. N. Armenise,
E. Armandillo*, I. McKenzie*

Optoelectronics Laboratory, Politecnico di Bari, Via Orabona 4, 70125 Bari, Italy
Tel: +39 080 5963404, Fax: +39 080 5963410, e-mail: c.ciminelli@poliba.it

(*) European Space Agency/European Space Research and Technology Centre (ESA/ESTEC),
Nordwijk, The Netherlands

Abstract—Recent results obtained on integrated optical gyroscopes are presented in this paper. The sensors configuration, based on high-Q resonators both in silica-on-silicon and InP technologies, is discussed and the estimation of the resonators performance through an accurate optical characterization is reported. On the basis of the numerical and experimental achievements, we demonstrate that resonant micro optical gyros can potentially exhibit resolution values in the range 1-10 °/h, which is demanded by several emerging space applications.

Keywords - on-board data handling; optical link; space photonics; optoelectronics.

I. INTRODUCTION

Autonomous navigation is a key functionality in a lot of space systems such as attitude and orbit control systems (AOCSs) of satellites and inertial measurement units (IMUs) of rovers for extraterrestrial exploration [1]. In the last decade, miniaturization of those systems has been identified as a crucial goal of R&D activities in the field of space technologies. So the interest toward compact and low-power inertial navigation sensors, such as gyroscopes, accelerometers, sun sensors, star trackers and magnetometers, is constantly growing [2].

Since its performance critically influences the system, the gyroscope is one of the key sensors of IMUs and AOCSs and its miniaturization is currently attracting an increasing research effort. One of the results of this effort has been the ESA-funded development of a 3-axis MEMS vibratory gyroscope with a mass of 0.75 Kg, a volume $< 1000 \text{ cm}^3$, and a power consumption $< 4 \text{ W}$ [3]. The target applications of that sensor, which is a coarse rate gyro, are those ones requiring resolution values $> 10 \text{ °/h}$, such as fault/failure detection [4].

An alternative way for gyros miniaturization is the scaling of conventional optical gyroscopes, i.e., the ring laser gyro (RLG) and the fiber optic gyro (FOG), which currently cover a wide performance range (resolution from 0.01 to 10 °/h) and are well established inertial sensors for space, routinely used in AOCSs of telecom and earth observation satellites.

Integrated optical technologies have allowed the demonstration of both micro-scale devices with outstanding performance [5] and integrated circuits including hundreds of active/passive optical components monolithically integrated on the same chip [6]. Therefore those technologies are crucial for the development of new generation optical gyroscopes with resolution $\leq 10 \text{ °/h}$ and mass, volume and power consumption comparable to those of MEMS angular velocity sensors [7].

At the beginning of '80s, two innovative integrated optical gyroscopes were envisaged and patented [8-9]. They are based on a planar guided-wave cavity supporting two counter-propagating resonant modes whose resonance frequencies are equal when the device is at rest, while suffer from a splitting induced by the Sagnac effect [10] when the cavity rotates. In integrated optical gyros based on semiconductor ring lasers (SRLs) [11-13], the resonant waves are generated within the cavity acting as sensing element while in resonant micro optical gyros (RMOGs) [14-15] the resonator is passive and it is excited by an external narrow-linewidth laser.

SRL-based angular velocity sensors have a very small area (footprint $< 1 \text{ cm}^2$) and can be easily integrated on a single chip but their performance is limited by backscattering and mode competition within the active cavity. Although less compact and with a more complex configuration, RMOGs are immune from those physical effects and so they are considered ideal candidates for novel optoelectronic gyros.

RMOGs resolution strongly depends on the cavity size, affecting the sensor scale factor, and the resonator quality factor Q which should be both maximized. Therefore high-Q large-area resonators manufactured by low-loss technologies (e.g., glass, silica-on-silicon) [15-16] are usually the basic building block of those sensors.

RMOGs have recently reached good compactness and interesting values of minimum detectable angular velocity (several hundreds of °/h with a resonator footprint = 6.3 cm^2 [17]). However, further improvements are needed to achieve the resolution range 1-10 °/h that is uncovered by silicon

MEMS gyros and appears to be realistic for RMOGs fabricated by the currently available technologies.

Selected numerical and experimental results, achieved in the framework of some ESA founded projects, on high-Q resonators properly designed and optimized for miniaturized gyros with target performance 1-10 °/h are presented in this paper. The configuration of RMOGs that we are developing is discussed, too.

II. SENSORS CONFIGURATION

The element sensitive to rotation in the basic configuration of an RMOG is the integrated resonator. The configuration includes a narrow linewidth laser generating the beam coming in the beam splitter (BS), two phase modulators and two acousto-optic frequency shifters for processing both optical beams coming out from the splitter, two photodiodes (D), and an electronic read-out unit [18,19].

The two beams coupled into the cavity excite two counter-propagating resonant modes having the same resonance order. Resonance frequencies of these modes are split by rotation and, according to the Sagnac effect, the difference between them (Δf) is proportional to the cavity angular rate Ω . The measurement of this difference, allowing the angular velocity estimation, is carried out by the closed-loop readout optoelectronic system which is based on the phase modulation spectroscopy [20] and includes the two photodiodes, the optoelectronic (OE) processing unit, whose key element are the modulators and the frequency shifters, and the electronic unit providing the sensor output and the two feedback electric signals controlling the OE processing unit.

The shot-noise limited resolution $\delta\Omega$ of RMOGs is given by:

$$\delta\Omega = \frac{f_s\sqrt{2}}{Q \cdot S} K \quad (1)$$

where

$$K = \sqrt{Bhf_s/\eta_{pd}P_{pd}} \quad (2)$$

f_s is the sensor operating frequency (= 193 THz, corresponding to an operating wavelength of 1.55 μm), S is the gyro scale factor defined as $\Delta f/\Omega$, B is the sensor bandwidth, h is Planck's constant, P_{pd} is the average power at the photodiodes input, and η_{pd} is the quantum efficiency of the two photodiodes.

The performance of the resonator in terms of the product $Q \cdot S$ determines the gyro resolution that can be enhanced by increasing Q and/or S .

Assuming $B = 1$ Hz, $\eta_{pd} = 0.9$, and $P_{pd} = 1$ mW, we can conclude that the achievement of the target resolution requires $Q \geq 10^6$ and resonator footprint of the order of 10 cm^2 .

Two technological approaches are available to implement the configuration of the RMOG above described, i.e., either the hybrid integration of optoelectronic components manufactured on different substrates or the monolithic integration of all components on a single chip. The former option allows the optimization of all the devices and the selection of the best technological platform for each of them, while the selection of the latter option enhances the device compactness and immunity to external disturbances (e.g., vibrations). The miniaturization of the electronic unit can be achieved by a properly designed ASIC (application-specific integrated circuit).

The best technology for the resonator is the silica-on-silicon technology, which allows propagation loss values very low (≤ 0.1 dB/cm) and consequently Q values exceeding 10^6 . Unfortunately that technology is not appropriate for the other optoelectronic components. Thus, if silica is selected for the high- Q cavity, the hybrid integration is the only option for the sensor fabrication.

InP technology seems to be the best choice for the monolithic integration of all gyro optoelectronic components but fabrication of high- Q InP integrated cavities is very challenging because InP waveguides usually exhibit propagation loss values > 1 dB/cm.

In the framework of the ESA IOLG (Integrated Optical Laser Gyroscope) project, a silica-on-silicon resonator with a footprint of 20 cm^2 was designed, optimized and fabricated. Some features of this resonator are described in the next Section.

The alternative approach of the gyro monolithic integration in InP PICs technology has been evaluated during an ESA-funded PhD and the demonstration of InP resonators with Q values of the order of 10^6 (about one order of magnitude more than the state-of-the-art) in one of the task of the ESA MiOS (Micro Optical angular velocity Sensor) project which is currently ongoing.

Recent results on the two fabricated resonators and the gyros based on them are reported in the following subsections.

III. SILICA RESONATOR

The silica-on-silicon resonator, fabricated by CIP (Centre for Integrated Photonics, Ipswich, UK), has a 3-loop spiral configuration and is evanescently coupled to two straight bus waveguides. The spiral length is 42 cm.

The cavity is thermally stabilized by a Peltier cell, packaged, and fiber pigtailed. It has been optically characterized by the setup shown in Fig. 1. A tuneable laser operating at 1.55 μm and having a linewidth less than 10 kHz, the laser controller connected to a computer, two photodiodes, a polarization controller, a signal generator, and an oscilloscope are the setup components.

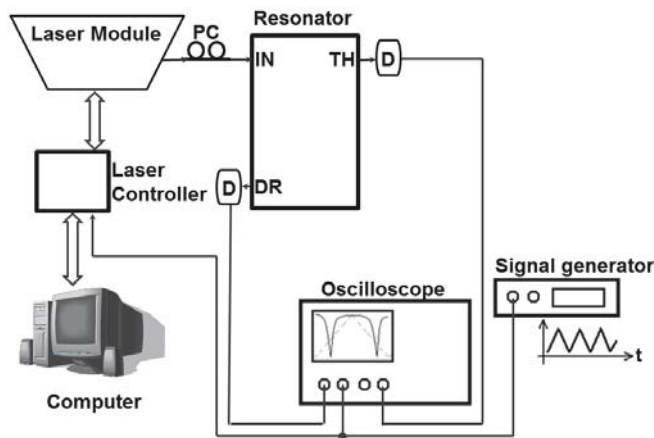


Figure 1. Characterization set-up for the estimation of the silica resonator spectral response (PC: polarization controller, IN: input port, TH: through port, DR: drop port).

For the spectral response measurement, the laser emission frequency has been linearly tuned by applying to the laser controller a triangular waveform generated by the signal generator. The electrical signal generated by the photodetector is acquired by the oscilloscope and then processed. Normalized spectral responses at both through and drop port have been derived. The resonance depth is 6.2 dB at the through port and 8.8 dB at the drop port. The resonator full width at the half maximum (FWHM) is 120 MHz and the free spectral range is 500 MHz. Therefore the cavity quality factor Q is 1.5×10^6 and its finesse is 4.2. The agreement between those experimental results and our theoretical predictions [21] obtained by a very accurate model is very good.

We have evaluated the thermal drift of the resonance frequency in two operating conditions, i.e. when the Peltier cell is not supplied and when it is supplied. In the former condition, the resonance frequency drift is about 200 to 400 kHz/s, while in the latter the drift decreases down to 20 kHz/s.

IV. INP RESONATOR

The InP cavity, shown in Fig. 3 (a), has a circular shape with a radius of 1.3 cm and a total length of 8.16 cm. It is evanescently coupled to just one straight bus waveguide. The configuration including one bus has been preferred to the one with two buses because the former exhibits a higher quality factor. To assure an appropriate uniformity of the technological process, the radius value has been chosen so that the cavity fits in $\frac{1}{4}$ of the 3-inch InP wafer.

An InGaAsP/InP rib waveguide with etch depth = 300 nm and width = 2000 nm has been selected for the device. The 1 μm thick InGaAsP guiding layer has the band-gap wavelength = 1.06 μm . The quasi-TE mode (see Fig 4 (b)) supported by the guiding structure exhibits a confinement factor exceeding 80 % and a propagation loss, estimated by the 3D model proposed in [22], in the range 0.5 to 0.8 dB/cm.

To enhance the fiber/waveguide coupling, a taper has been designed and manufactured at the two ends of the straight waveguide. The waveguide width has been tapered up to 8000 nm (core diameter of a standard single mode fiber) and the taper length is 0.2 mm. Optical propagation within the taper has been simulated by the 3D BPM (Beam Propagation Method). Loss due to the propagation within the taper is less than 1 % and the overlap integral between the taper output field and the field of a standard single mode fiber is equal to 22 %.

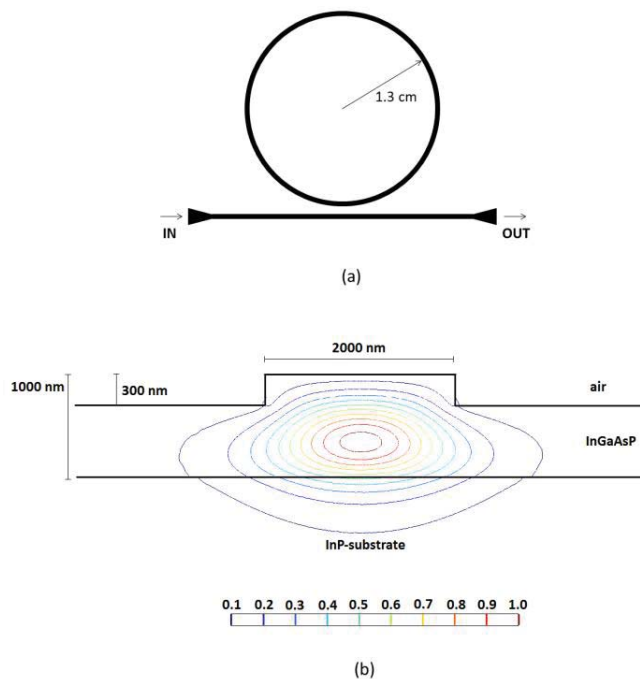


Figure 3. (a) Configuration of the fabricated InP resonator. (b) Quasi-TE mode supported by the selected InGaAsP/InP rib waveguide. Level curves relevant to the normalized squared module of the electric field are shown.

The gap between the ring resonator and the straight bus waveguide, which determines the efficiency of the bus/cavity coupler, has been designed by imposing a resonance depth of 8 dB. We have calculated both the coupler efficiency value allowing to fulfill this constraint (η_{opt}) and the relevant value of the gap between the ring and the straight bus waveguide (g_{opt}). We have evaluated the dependence of η_{opt} and g_{opt} on the waveguide propagation loss α (we varied α in the range $0.5 \div 1$ dB/cm) by using the Coupled Mode Theory. The optimized values of the gap and the coupler efficiency vs. α are shown in Fig. 4 by a two y-axis plot. As α increases, the optimum coupler efficiency increases and consequently g_{opt} decreases.

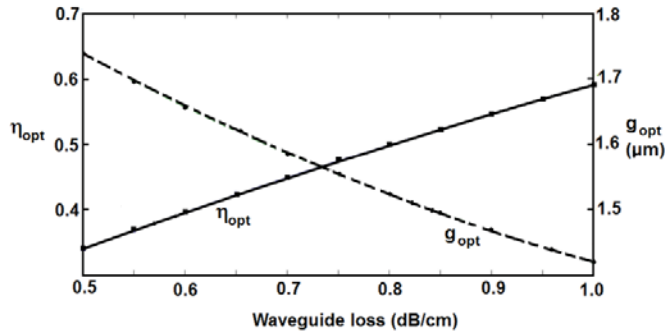


Figure 4. Dependence of the optimum coupler efficiency and the optimum gap value on the waveguide loss.

Since the numerically predicted propagation loss is in the range $0.5 \div 0.8$ dB/cm, to optimize the design of the sensor we have considered four different values of the gap between the bus and the ring: $g_1 = 1.739 \mu\text{m}$ (relevant to $\alpha = 0.5$ dB/cm), $g_2 = 1.620 \mu\text{m}$ (relevant to $\alpha = 0.65$ dB/cm), $g_3 = 1.524 \mu\text{m}$ (relevant to $\alpha = 0.8$ dB/cm), and $g_4 = 1.444 \mu\text{m}$ (relevant to $\alpha = 0.95$ dB/cm).

The four InP resonators with the selected values of the gap have been fabricated at the Fraunhofer Institute for Telecommunication, Heinrich-Hertz-Institut, Berlin, by using metal-organic vapor-phase-epitaxy, standard photolithography and reactive ion etching [23]. Preliminary optical characterization shows that the best performing resonator is that one with gap = $1.524 \mu\text{m}$, which exhibits a quality factor of about 10^6 and resonance depth = 7 dB.

V. SENSOR RESOLUTION

As shown by Eq. (1), RMOGs resolution depends on the resonator quality factor, the sensor scale factor, and the average power at the photodiodes. Footprint, S, Q and the product Q·S for both the silica resonator and the InP one is reported in Table 1.

TABLE I. FEATURES OF RMOGS BASED ON THE SILICA RESONATOR AND THE INP ONE.

	RMOG based on the silica resonator	RMOG based on the InP resonator
Resonator footprint	20 cm ²	7 cm ²
Sensor scale factor	2.88×10^4	1.68×10^4
Resonator quality factor	1.5×10^6	1×10^6
Q·S	4.32×10^{10}	1.68×10^{10}

The resolution of gyros including the two cavities depends on P_{pd} that can be maximized by reducing optical beam loss in its path from the laser to the photodetectors.

The dependence of $\delta\Omega$ on P_{pd} for the RMOGs based on both the silica-on-silicon cavity and the InP one is shown in Fig. 5. Log scale has been used for both axes. The resolution is enhanced by the P_{pd} increase and it is better for the gyro based on the silica resonator, which exhibits a larger footprint and quality factor. The target resolution ($10 \text{ }^\circ/\text{h}$) is achieved for P_{pd} equal to about 2 mW and 14 mW for the sensors based on the silica cavity and the InP one, respectively. Photodiodes compatible with those P_{pd} values, having saturation power values up to 20 mW, are available on the market.

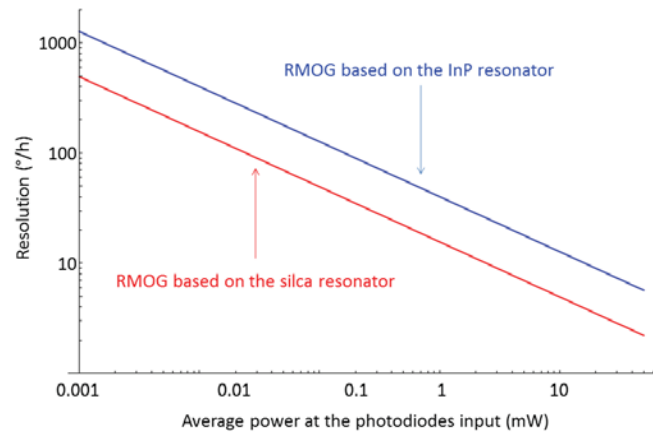


Figure 5. Resolution of RMOGs based on the silica resonator and the InP one vs. average power at the photodiodes input.

VI. CONCLUSIONS

Experimental results on two resonators properly designed for gyro applications and fabricated in the framework of two recent ESA-funded projects are discussed in this paper. The silica spiral resonator with a length of 42 cm has a quality factor of 1.5×10^6 and a finesse of 4.2. The circular InP cavity, having a shorter length (= 8.16 cm), exhibits a quality factor of 10^6 . Numerical simulations based on those achievements show that both RMOGs that we are developing can be used for the application domains demanding a resolution of 1-10 $^\circ/\text{h}$, such as attitude control of telecom satellites and autonomous navigation of rovers for extraterrestrial exploration.

ACKNOWLEDGEMENTS

This work has been partially funded by the European Space Agency (ESA) under MiOS project 4000102311/10/NL/PA. The authors would like to thank Dr. Francisco Soares for the InP ring resonator fabrication and for his valuable comments.

REFERENCES

- [1] P. Fortescue, J. Stark, G. Swinerd, Eds., *Spacecraft systems engineering*. Chichester, UK: John Wiley and Sons, 2003.
- [2] D. Titterton, J. Weston, *Strapdown Inertial navigation Technology*, Stevenage. UK: The Institution of Electrical Engineers, 2004.
- [3] Datasheet of the SiREUS MEMS Rate Sensors available at <http://www.sea.co.uk/Docs/aerospace/Aerospace%20data%20sheets/ME MS%20DATASHEET%20MAY08%20rev.pdf>
- [4] M. Hartree, P. Hutton, B. Olivier, D. Temperanza, "The European Silicon MEMS Rate Sensor takes to Space," presented at Guidance and Control Conference, 2011.
- [5] E. J. Murphy, *Integrated Optical Circuits and Components: Design and Applications*. Boca Raton, FL: Taylor and Francis, 1999.
- [6] R. Nagarajan et al., "Large-Scale Photonic Integrated Circuits," *IEEE J. Sel. Topics in Quant. Electron.*, vol. 11, pp. 50 - 65, 2005.
- [7] C. Ciminelli, F. Dell'Olio, C. E. Campanella, M. N. Armenise, "Photonic technologies for angular velocity sensing," *Advances in Optics and Photonics*, vol. 2, pp. 370 - 404, 2010.
- [8] O. Kenji, "Semiconductor ring laser gyro," *Japanese patent # JP 60,148,185*, filed in 1984, published in 1985.
- [9] A. W. Lawrence, "Thin film laser gyro," *US patent # 4,326,803*, filed in 1979, published in 1982.
- [10] G. Sagnac, "L'èther lumineux démontré par l'effet du vent relatif d'èther dans un interféromètre en rotation uniforme," *C. R. Acad. Sci.*, vol. 95, pp. 708 - 710, 1913.
- [11] M. Armenise, P. J. R. Laybourn, "Design and simulation of a ring laser for miniaturised gyroscopes," *Proc. SPIE*, vol. 3464, pp. 81 - 90, 1998.
- [12] M. N. Armenise, V. M. N. Passaro, F. De Leonardis, M. Armenise, "Modeling and design of a novel miniaturized integrated optical sensor for gyroscope applications," *J. Lightwave Technol.*, vol. 19, pp. 1476 - 1494, 2001.
- [13] M. N. Armenise, M. Armenise, V. M. N. Passaro, F. De Leonardis, "Integrated optical angular velocity sensor," *European Patent # 1219926*, filed in 2002, published in 2010.
- [14] C. Ciminelli, F. Peluso, M. N. Armenise, "A new integrated optical angular velocity sensor," *Proc. SPIE* **5728**, 93-100 (2005).
- [15] K. Suzuki, K. Takiguchi, K. Hotate, "Monolithically integrated resonator microoptic gyro on silica planar lightwave circuit," *J. Lightwave Technol.*, vol. 18, pp. 66 - 72, 2000.
- [16] G. Li, K. A. Winick, B. R. Youmans, E. A. J. Vikjaer, "Design, fabrication and characterization of an integrated optic passive resonator for optical gyroscopes," presented at Institute of Navigation's 60th Annual Meeting, 2004.
- [17] H. Mao, H. Ma, Z. Jin, "Polarization maintaining silica waveguide resonator optic gyro using double phase modulation technique," *Optics Express*, vol. 19, pp. 4632 - 4643, 2011.
- [18] C. Ciminelli, F. Dell'Olio, C. E. Campanella, M. N. Armenise, "Numerical and experimental investigation of an optical high-Q spiral resonator gyroscope," presented at 14th International Conference on Transparent Optical Networks (ICTON), 2012.
- [19] F. Dell'Olio, C. Ciminelli, M. N. Armenise, F. M. Soares, W. Rehbein, "Design, fabrication, and preliminary test results of a new InGaAsP/InP high-Q ring resonator for gyro applications," presented at 24th International Conference on Indium Phosphide and Related Materials, 2012.
- [20] H. Ma, X. Zhang, Z. Jin, C. Ding, "Waveguide-type optical passive ring resonator gyro using phase modulation spectroscopy technique," *Opt. Eng.* **45**, 080506 (2006).
- [21] European Space Agency (ESA), IOLG project 1678/02/NL/PA, Final Report, Dec. 2008.
- [22] C. Ciminelli, V. M. N. Passaro, F. Dell'Olio, and M. N. Armenise, "Three-dimensional modelling of scattering loss in InGaAsP/InP and silica-on-silicon bent waveguides," *J. of the European Optical Society - Rapid Publications*, vol. 4, 09015, 2009.